-Supporting Information-

A branched electrode based electrochemical platform: towards new label-free and reagentless simultaneous detection of dual proteins

Fen-Ying Kong, Bi-Yi Xu, Ying Du, Jing-Juan Xu and Hong-Yuan Chen*

State Key Laboratory of Analytical Chemistry for Life Science, School of Chemistry and Chemical Engineering, Nanjing University, Nanjing 210093, China.

Tel/ Fax: +86-25-83597294; E-mail: xujj@nju.edu.cn

Experimental section

Materials

CEA and AFP standard grade antigens, anti-CEA and anti-AFP antibodies were purchased from Linc-Bio Science Co. (Shanghai, China). Carboxyl graphene sheet (CGS) dispersion (the content of carboxyl >5 wt%) was obtained from Nanjing XFNANO Materials Tech Co., Ltd., (Nanjing, China). N-(3-dimethylaminopropyl)-N'-ethyl-carbodiimide hydrochloride (EDC), N-hydroxysuccinimide (NHS), bovine serum albumin (BSA) were purchased from Sigma (St. Louis, USA). MB, potassium ferricyanide ($K_3Fe(CN)_6$), ferric chloride ($FeCl_3 \cdot 6H_2O$) came from Shanghai Chemical Reagent Company (Shanghai, China). ITO-coated (thickness: 100 nm; resistance: 10 Ω sqr^{-1}) aluminosilicate glass slides were purchased from CSG (Shenzhen, China). Serum specimens provided by Gulou Hospital (Nanjing, China) were stored at 4 °C. All other chemicals were of analytical grade. Ultrapure water (18.2 $M\Omega cm^{-1}$) was obtained from a Milli-Q water purification system and used in all experiments. Phosphate-buffered saline (PBS, 0.1 mol L^{-1}) at various pH values was prepared by mixing a stock standard solution of NaH_2PO_4 and Na_2HPO_4, which was used as the measuring buffer, and then adjusting the pH with 0.1 mol L^{-1} NaOH and H_3PO_4.

Apparatus

All electrochemical measurements were performed on a CHI 760 C electrochemical workstation (Shanghai, China). A conventional three-electrode system was used with an Ag/AgCl electrode as the reference electrode, a platinum wire as the counter electrode, and a modified ITO electrode as the working electrode. All potentials reported in the text were with respect to the Ag/AgCl (sat. KCl) reference electrode. The scanning electron micrographs were taken with scanning electron microscope (SEM, S-3000 N, Tokyo, Japan). Ultraviolet–visible (UV–vis) spectrophotometric measurements were carried out using a UV–3600 spectrophotometer (Shimadzu, Japan).

Device fabrication

The ITO electrode design comprising of two circular areas (each 2 mm in diameter, named as W_1 and W_2)

joined to a rectangular area for the electrical contact. Fig.S-1 shows the typical photograph of branch electrode. The ITO electrode fabrication was based on photolithography. Firstly, the ITO on the surface of a glass slide was covered by a thin layer of photoresist with the thickness of 100 μm. After baking, the electrode pattern on the mask was transferred to the thin layer of the photoresist by UV exposure. Then the glass slide was immersed into 10 mmol L^{-1} NaOH for 1 min followed by rinsing with ultrapure water. The immersion and rinsing steps were repeated for at least 5 times to wash away the unattached photoresist. Then the slide was immersed into the ITO etchant ($FeCl_3$: HNO_3 : HCl = 0.5 mol L^{-1} : 1 mol L^{-1} : 1 mol L^{-1}) for 30 min at room temperature to remove exposed ITO. After rinsing with water, the remaining photoresist was removed by ethanol. Then the ITO electrode was washed by sonification in water and ethanol each for 10 min, followed by immersion in a boiling solution of 2 mol L^{-1} KOH in 2-propanol for 20 min. Finally, the ITO electrode was rinsed thoroughly with ultrapure water and dried under nitrogen flow.

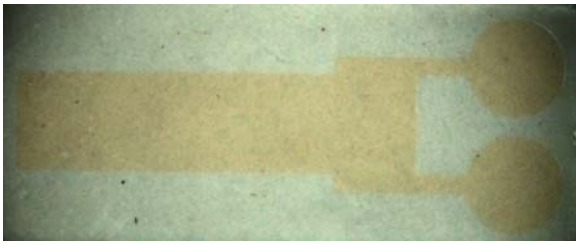

Fig.S-1 A typical photograph of branch electrode.

Preparation of BSA/anti-CEA/CGS-MB bioconjugates

For preparation of BSA/anti-CEA/CGS-MB bioconjugates, we firstly synthesized CGS-MB nanocomposite. Briefly, after ultrasonication for 40 min at room temperature, 2 mL of CGS dispersion (0.5 mg mL^{-1}) was mixed with 2 mL MB solution (1 m mol L^{-1}) and stirred vigorously for 24 h. Finally, CGS-MB nanocomposite was obtained by removing the non-integrated MB away through centrifugation and washing with ultrapure water. Subsequently, the BSA/anti-CEA/CGS-MB bioconjugate was prepared as follows: the as-prepared CGS/MB nanocomposite was dispersed in 2 mL water. Then 2 mL of 20 μg mL^{-1} EDC and 10 μg mL^{-1} NHS solutions were added into this dispersion and reacted for 1 h. After centrifugation, 1 mL of 100 μg mL^{-1} anti-CEA was added into the dispersion. The mixture was set on a shaker for 12 h followed by centrifugation. The unreacted covalent-active surface groups were subsequently blocked by reaction with 1% (w/w) BSA at room temperature for 2 h. Finally, the resulting bioconjugates were washed with PBS and then re-dispersed in 1 mL buffer and stored at 4 °C before use.

Synthesis of BSA/anti-AFP/CGS-PB bioconjugates

CGS-PB nanocomposite was synthesized via an in situ reduction process. Typically, 2 mL of CGS dispersion (0.5 mg mL^{-1}) was added into 2 mL pH 1.5 (adjust with HCl) aqueous solution containing 10 mmol L^{-1} $FeCl_3 \cdot 6H_2O$ and 10 mmol L^{-1} $K_3Fe(CN)_6$. After stirring for 2 h, the color of the mixture gradually changed from yellow brown to dark cyan, suggesting the formation of CGS-PB nanocomposite. The nanocomposite was collected by centrifugation and washed with ultrapure water for several times, and redispersed in 2 mL of water

for further use. Anti-AFP was attached to CGS using an EDC/NHS amidization protocol. Briefly, the as-prepared CGS-PB dispersion was mixed with 2 mL of EDC/NHS solutions (20 μg mL^{-1} EDC and 10 μg mL^{-1} NHS) and activated for 1 h. Then the mixture was centrifuged and rinsed repeatedly to remove excessive EDC and NHS. Subsequently, 1 mL of anti-AFP solution (100 μg mL^{-1}) was added into the dispersion, and the mixture was allowed to react for 12 h with gentle shaking. After centrifugation, the resulting mixture was treated with 1% (w/w) BSA solution for 2 h to block possible remaining active sites and avoid the nonspecific binding. Following centrifuged and washed, the resulting BSA/anti-AFP/CGS-PB bioconjugates were stored at 4 °C in refrigerator until use.

Immunoassay protocol and electrochemical measurement

For the fabrication of immunosensor, 2 μL of 0.1 mg mL^{-1} BSA/anti-CEA/CGS-MB and 2 μL of 0.1 mg mL^{-1} BSA/anti-AFP/CGS-PB dispersions were cast onto the W_1 and W_2 of the ITO surface, respectively, and dried at room temperature. After rinsing thoroughly with PBS, the modified electrode was immersed in 0.2 mL incubation solution containing various concentrations of CEA and AFP for 15 min at room temperature, then washed carefully with PBS.

Prior to the electrochemical measurement, the ITO electrode was sealed by a tape in order to exposure only the W_1 and W_2 of ITO electrode to the solutions. Then the resulting electrode was placed in the detection cell with 1 mL of PBS (pH 7.0), and DPV responses of the immunosensor were recorded from 0.6 V to −0.7 V with the pulse amplitude of 50 mV and the pulse width of 50 ms. The detection was based on the current changes of redox probe MB and PB before and after the corresponding antigen-antibody reaction, respectively. After the antigen–antibody reaction, the response current of MB and PB decreased due to the formation of immunocomplex, which was directly proportional to the concentration of corresponding antigen. According to the linear relationship, the detection of CEA and AFP in the sample solution can be assessed quantitatively.

Characteristics of the CGS-MB and CGS-PB nanocomposite

Fig.S-2 shows the typical SEM images of the CGS, CGS-MB and CGS-PB nanocomposite. As shown in Fig. S-2A, CGS presents a typical flake-like shape with slight wrinkles on the surfaces. The scraggy surface can provide a large surface area for the assembly of nanoparticles or biomolecules. The conjugation of MB through π–π stacking interactions has the morphology similar to that of CGS (Fig. S-2B). Fig. S-2C displays the SEM image of the CGS-PB nanocomposites. It can be clearly observed that many PB nanoparticles are typically adhered to the CGS surface, indicating the formation of CGS/PB nanocomposite.

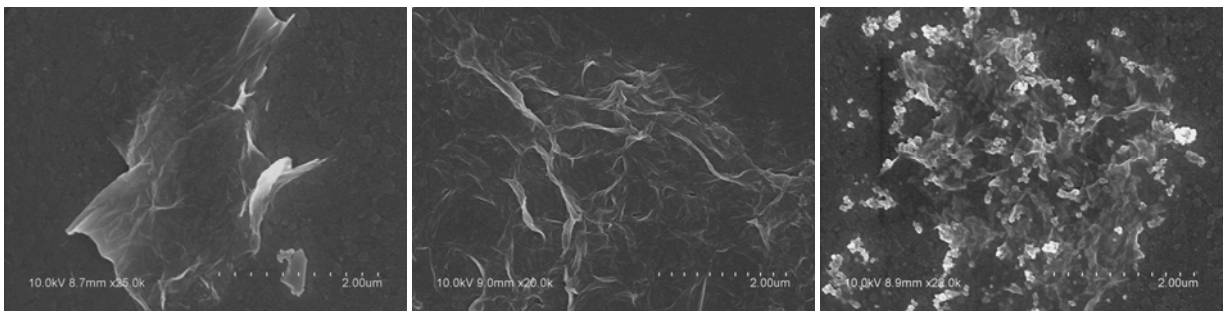

Fig.S-2. SEM image of CGS (A), CGS-MB (B) and CGS-PB nanocomposite (C)

To further demonstrate the formation of CGS-MB and CGS-PB nanocomposites, UV–vis absorption spectrum was used to characterize the synthesized nanostructures. Fig. S-3A shows the spectrum obtained by the CGS. As can be seen, the CGS dispersion solution exhibits a strong absorption band at 230 nm and a shoulder at 300 nm, attributing to л–л* transitions of carbon–carbon bonds and n–л* transitions of carboxyl bonds, respectively [1]4. In this study, MB was directly adsorbed onto CGS through л–л stacking interactions. Fig. S-3B shows the spectrum of CGS-MB nanocomposite. Two distinct absorption bands around 290 and 610 nm are observed, which are ascribed to MB. The difference in absorption spectrum between CGS-MB and CGS confirmed that MB molecules are adsorbed onto CGS to form CGS-MB nanocomposite. CGS-PB nanocomposite was prepared via an in situ reduction of $FeCl_3$ and $K_3Fe(CN)_6$ solution. The corresponding UV–vis absorption spectrum is shown in Fig. S-3C. The characteristic absorption band of PB at 300 nm and 750 nm is also observed, indicating that CGS-PB nanocomposite is successfully formed. These observations are consistent with the reported literature [2].

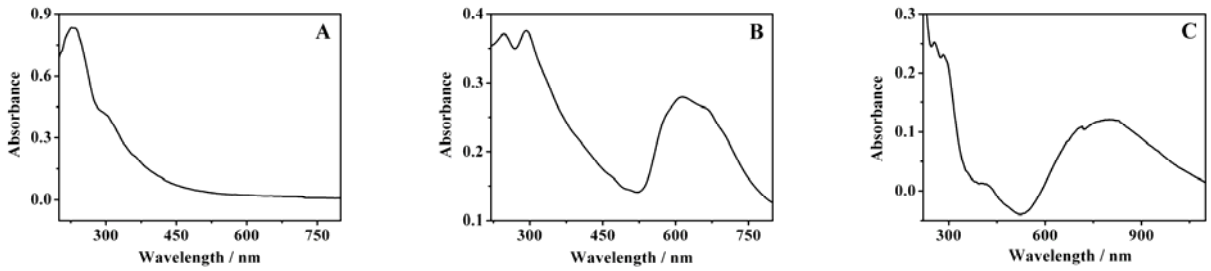

Fig.S-3. UV–vis absorption spectrum of CGS (A), CGS-MB (B) and CGS-PB nanocomposite (C).

Electrochemical characteristics of the different electrodes

The DPV of the differently modified electrodes in a 0.1 mol L^{-1} PBS (pH 7.0) is presented in Fig. S-4. No voltammetric peak was observed at the bare ITO electrode in the working potential range as a lack of any redox probes (Fig. S-4a). After the BSA/anti-CEA/CGS-MB and BSA/anti-AFP/CGS-PB dispersions were cast onto the W_1 and W_2 of ITO electrode surface, the resulting electrode showed two pronounced redox peaks at -0.33 V and 0.24 V, respectively, which indicated that the MB and PB in the bioconjugates retained the good redox properties (Fig. S4-b). Subsequently, when the resulting immunosensor was incubated with a mixture solution of CEA and AFP, a simultaneous and significant decrease of the peak currents of MB and PB were observed (Fig. S-4c). The reason is that the antigen–antibody immunocomplex on each work area acts as the inert electron and mass-transfer blocking layer, which greatly inhibited the corresponding reaction on the electrode surface. From these results, it could be seen that the designed electrode could be used for the simultaneous detection of CEA and AFP.

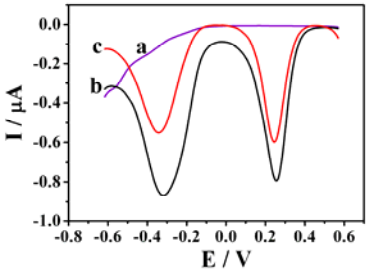

Fig. S-4. DPV of the different modified electrodes in pH 7.0 PBS. (a) bare ITO electrode, (b) BSA/anti-CEA/CGS-MB and BSA/anti-AFP/CGS-PB modified electrode, (c) CEA/BSA/anti-CEA/CGS-MB and AFP/BSA/anti-AFP/CGS-PB modified electrode (20 ng mL^{-1} CEA and 20 ng mL^{-1} AFP).

Optimization of immunosensor response

It is well known that the pH value of the measuring solution has a profound effect on the performance of immunosensor. It greatly affected both the activity of the immobilized protein and the electrochemical behavior of the MB and PB mediator. The influence of pH on the DPV peak current was investigated in the range from 4.0 to 9.0 (Fig. S-5A). The results indicted that the MB reduction peak current decreased with an increase of pH (curve a), while the PB reduction peak current increased with increasing pH value when pH<5.5 (curve b). Considering that PB is not very stable at pH above 7 and the activity of the antibody or antigen is decreased at relatively high and low pH. Therefore, pH 7.0 was chosen as a compromise in our experiments.

Incubation temperature and incubation time also affected the performance of the immunosensors. To make the immunosensor more feasible for practical purposes, the room temperature was chosen for the antigen–antibody interaction. In the incubating solution, when the analyte antigens reached the antibodies immobilized on the electrode surface of the immunosensor, it would take some time for the contacting species to form immunocomplexes. The effect of the incubation time on the peak current of the immunosensor was investigated. As shown in Fig. S-5B, the peak current of PB (curve a) and MB (curve b) rapidly decreased with the increase of incubation time, and reached a plateau after 15 min, indicating an equilibration state arrived. Therefore, 15 min was selected as the incubation time for the subsequent assays.

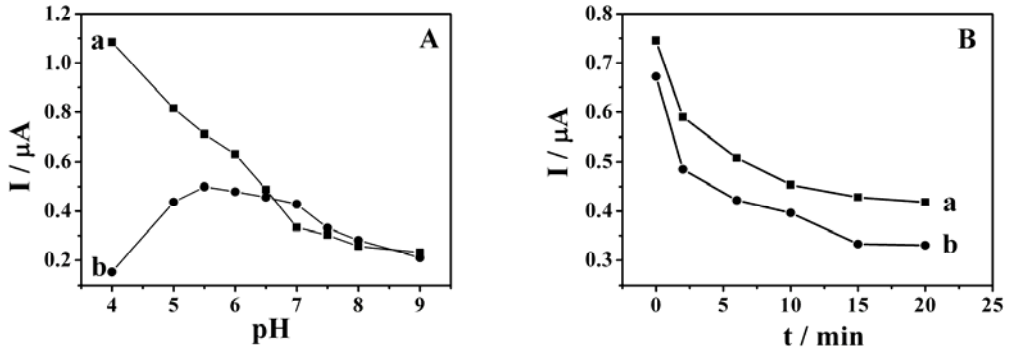

Fig. S-5. Effect of pH (A) and incubation time (B) on the peak currents of the immunosensor toward 50 ng mL^{-1} CEA and AFP.

Immunosensing in real human serum

Table S1 Recovery tests for CEA and AFP in human serum.

Sample number	Standard value (ng/mL)		Found value (ng/mL)		Recovery (%)	
	CEA	AFP	CEA	AFP	CEA	AFP
1	1.00	1.00	1.10	1.03	110	103
2	5.00	5.00	5.34	5.22	107	104
3	10.0	10.0	9.58	9.86	95.8	98.6
4	20.0	20.0	19.5	21.4	97.5	107
5	40.0	40.0	39.7	36.8	99.3	92.0

References.

1. J. I. Paredes, S. Villar-Rodil, A. Martinez-Alonso and J. M. D. Tascon, *Langmuir*, 2008, **24**, 10560.
2. J. D. Qiu, M. Xiong, R. P. Liang, J. Zhang and X. H. Xia, *J. Nanosci. Nanotechnol.*, 2008, **8**, 4453.